Ground and Excited-State Acetic Acid Catalyzed Double Proton Transfer in 2-Aminopyridine[†]

Fa-Tsai Hung,*[,‡] Wei-Ping Hu,*[,§] Tsung-Hui Li,[§] Chung-Chih Cheng,[∥] and Pi-Tai Chou*[,⊥]

National Hu-Wei Institute of Technology, 632, Yunlin, Taiwan, R.O.C., Department of Chemistry and Biochemistry, National Chung-Cheng University, 621, Chia Yi, Taiwan, R.O.C., Department of Chemistry, Fu-Jen Catholic University, 242, Taipei, Taiwan, R.O.C., and Department of Chemistry, National Taiwan University, 106, Taipei, Taiwan, R.O.C.

Theoretical calculations on the ground and excited state double proton transfer in the 2-aminopyridine (2AP)/ acetic acid dual hydrogen-bonded system have been performed. Comparisons have been made between thermodynamic parameters deduced from the theoretical approach and those extracted by absorption and fluorescence titration studies. Incorporating the electron correlation, only one transition geometry was resolved in the ground state. The barrier for the 2(*1H*)-pyridinimine/acetic acid → 2AP/acetic acid ground-state reverse proton transfer was estimated to be as small as 1.60 and 0.40 kcal/mol at MP2/6-31G(d′,p′) and B3LYP/6-31+G(d′,p′) levels, respectively. The first excited singlet state of the 2AP/acetic acid system possesses a $\pi\pi^*$ configuration, in which two transition-state geometries were resolved for the 2AP/acetic acid → 2(*1H*)-pyridinimine/acetic acid double proton transfer at the CIS level. The barriers were estimated to be 9.48 and 8.67 kcal/mol (relative to the reactant) using the CIS/6-31+G(d′,p′) method, whereas two barriers merge to a single, wide barrier upon inclusion of the zero-point energy. In both ground and excited states, the sequence of the asynchronous double proton transfer correlates with the hydrogen-bonding strength. The results provide a theoretical basis for picosecond dynamics of the 2AP/acetic acetic system recently reported by Ishikawa et al. (*J. Phys. Chem. A* **2002,** *106,* 2305). Similarities and differences between the theoretical approaches and the experimental results were discussed.

1. Introduction

Spectroscopy and dynamics of the host/guest types of the excited-state proton-transfer reaction have long received considerable attention owing to their fundamental basis and biological interests.[1] Recent prototypes include 7-azaindoles,[2−13] lumichrome,[14] hydroxyquinolines,[15] 2-(2′-pyridyl)indoles,[16,17] mono- and di-pyrido[2, 3a]carbazoles,[18,19] β-carbolines,[20−23] and 2-aminopyridines,[24−26] in which the excited-state proton-transfer tautomerism is mediated by either self-association or adding guest molecules (including solvents) upon forming host/guest types of hydrogen-bonding complexes.

One of the fundamental interests regarding the host/guest type of double proton transfer is in whether the mechanism incorporates the concerted or stepwise pattern. A well-known model should be ascribed to 7-azaindole (7AI), in which the excited-state double proton transfer (ESDPT) takes place through forming a precursor of the dual hydrogen-bonding (HB) dimer. Intensive studies on the 7AI dimer have been performed, and the results have shown certain controversies in experimental[4,5] and theoretical[6,7] approaches from the viewpoint of a concerted versus stepwise mechanism. Recently, picosecond dynamics on another host/guest system, the 2-aminopyridine (2AP)/acetic acid complex, have been investigated by Ishikawa et al.[26] Upon

exciting the dual HB 2AP/acetic acid complex, ESDPT takes place through the catalysis of acetic acid, resulting in an imine-like tautomer emission maximum at ∼420 nm (in cyclohexane). Through the analyses of the time-dependent spectral evolution, Ishikawa et al. were able to extract the cationic-like 2AP fluorescence ($\lambda_{max} \sim 360$ nm), which is otherwise unobtainable via the steady-state approach. The 5 ps decay dynamics of the transient cationic emission is similar to the rise component of the 420 nm tautomer emission. This, in combination with the irresolvable (≪5 ps) normal emission for the 2AP/acetic acid complex, led Ishikawa et al. to conclude the existence of an intermediate, i.e., a stepwise pattern, during the ESDPT reaction. Accordingly, the resolvable 5 ps rise time of the tautomer emission was ascribed to the second proton-transfer process, whereas the first-step proton transfer is too fast to be resolved by their streak camera detecting system.

Owing to the relatively simple hydrogen-bonded system, the 2AP/acetic acid complex should provide a reliable basis for the theoretical approaches on the mechanism of guest/host types of the ESDPT reaction. Although geometries as well as energetics of the stationary points for both 2AP/acetic acid normal and tautomer complexes have been performed via semiempirical calculations,[24] to our knowledge, ab initio calculations have not been reported, in particular the approaches regarding the potential energy surface along the proton-transfer reaction. Unlike the 7AI dimer possessing symmetric, dual hydrogen bonds, the 2AP/acetic acid complex consists of nonequivalent, dual hydrogen-bonding sites, of which the difference in the HB strength might render different insights into the ESDPT dynamics. In this study, ab initio approaches

---

Double Proton Transfer in 2-Aminopyridine

J. Phys. Chem. A, Vol. 107, No. 18, 2003 **3245**

to the double proton transfer of the 2AP/acetic acid system in ground and excited states have been performed. Comparisons have been made between thermodynamic parameters deduced from the theoretical approach and those extracted by comprehensive absorption and fluorescence titration studies. The results of ESDPT energetics in the excited state provide a theoretical basis to compare with recent picosecond dynamic results.[26]

2. Experimental Section

2.1. Measurements. Steady-state absorption and emission spectra were recorded by a Hitachi (U-3310) spectrophotometer and an Edinburgh (FS920) fluorimeter, respectively. Both wavelength-dependent excitation and emission response of the fluorimeter have been calibrated. To obtain the thermodynamic parameters of the HB association, we have carefully performed absorption and fluorescence titration studies where each data point was taken by averaging three to five measurements. The sensitivity for the absorption measurement is approximately 5×10^{-4} in absorbance under constant temperature ($\pm 0.1°C$) throughout the measurement.

2.2. Theoretical Approaches. The electronic structure calculation was performed using the Gaussian 98 program.[27] The geometry optimization was performed on the 2AP/acetic acid complex, transition state (TS), and the corresponding proton-transfer tautomer was preformed on the electronic ground state using the Hartree−Fock (HF),[28,29] MP2 theories,[30,31] hybrid density functional theories (DFT) B3LYP[32,33] with 6-31G(d′, p′) basis set,[27,34] and B3LYP with 6-31+G(d′, p′) basis set.[35] The geometry of these stationary points on the first electronic excited states ($\pi\pi^*$) was also calculated using the CI Singles (CIS)[29b,36] theory with 6-31G(d′,p′) and 6-31+G(d′,p′) basis sets. Time-dependent (TD)[37] B3LYP was also used to calculate the excited-state energies at the calculated stationary point geometry in the ground and the excited states. For comparison, the geometry and energetics of the 2AP monomer, its proton-transfer TS, and the tautomer were also calculated.

The enthalpy and free energy in the gas-phase was calculated from the thermodynamic data listed in the output of the Gaussian calculation without any scaling in vibrational frequencies. In addition, the harmonic approximation was applied in evaluating the vibrational contributions. The HB association energy, ΔH_{ac}, in the ground state was calculated as the change in the total molecular enthalpy for the conversion of the isolated monomers into the complex, which then incorporated with a counterpoise correction procedure[38−40] to correct certain inconsistencies because of the basis-set superposition error (BSSE). Accurate ab initio or DFT approaches using the SCRF methods (PCM, SCIPCM, etc.) to calculate the solvent−solute interaction for various complexes are very time-consuming processes on the basis of our current computing facility. Alternatively, a semi-empirical PM3-SM4 solvation model developed by Cramer and Truhlar[41,42] was applied to calculate the solvation energy. The solvation free energies were obtained with an AMSOL version 5.4 program[43] and then added to "gas-phase" energies obtained from the DFT method. This combination method has proven to reproduce the experimental results reasonably well.[44]

3. Results

3.1. Approaches in the Ground State. Figure 1 depicts the optimized geometry of the 2AP monomer in both normal and tautomer forms at the B3LYP/6-31+G(d′,p′) level of theory. Table 1 lists the ground-state thermodynamic parameters for 2AP monomer and 2AP/acetic acid complex in normal and tautomer states. The proton-transfer tautomer form of the 2AP
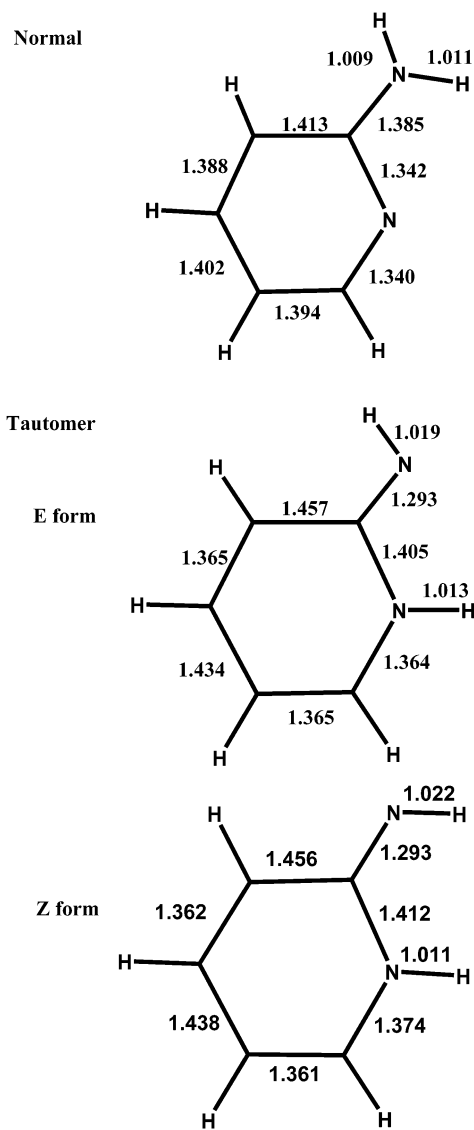
Figure 1. Geometry optimized structures (B3LYP/6-31+G(d′,p′) level) of the 2AP monomer in both normal and tautomer forms at the ground electronic state.

monomer, i.e., (E)-2(1H)-pyridinimine (see Figure 1), was calculated to be 14.06 kcal/mol higher in energy than the normal form. Another possible conformer of the proton-transfer tautomer, (Z)-2(1H)-pyridinimine (see Figure 1), was ~3 kcal/mol less stable than the (E)-2(1H)-pyridinimine form and, hence, is not of particular concern in this study. Hereafter, the abbreviation 2PI is used to denote the (E)-2(1H)-pyridinimine structure, whereas 2AP stands for the normal amino form throughout the text. The inclusion of a solvation free energy based on the PM3-SM4 model results in similar relative energies, in which 2AP is more stable than 2PI by 13.98 kcal/mol in cyclohexane.

Table 2 specifies several critical bond lengths at the optimized stationary-point geometries at various theoretical levels. Figure 2 depicts the geometry-optimized structure of the 2AP/acetic acid and 2PI/acetic acid complexes at the B3LYP/6-31+G(d′,p′) level of theory. Strong dual hydrogen-bonding formation in the 2AP/acetic acid complex was indicated by the short N(1)- - -H(8) and H(4)- - -O(5) distances of 1.675 and 1.897 Å, respectively. In comparison to the 2AP monomer (see Figure 1) significant changes in N(1)−C(2) and C(2)−N(3) bond distances of +0.01 and −0.03 Å, respectively, were found upon formation of the 2AP/acetic acid complex. The results correlate

TABLE 1: Ground-State Thermodynamic Parameters of 2AP Monomers and 2AP/Acetic Acid Complex Calculated by the B3LYP/6-31+G(d′,p′) Level of Theory at 298 K (in the Gas Phase) in Combination with the PM3-SM4 Method (in Cyclohexane)

	monomer			complex	
	2AP	2PI	acetic acid	2AP/acetic	2PI/acetic
enthalpy (hartree)	−303.56281	−303.54032	−229.04035	−532.62463	−532.61301
free energy (hartree)	−303.59845	−303.57588	−229.07327	−532.67645	−532.66485
$\triangle E_{cp}$(BSSE) (kcal/mol)[a]				−0.66	−0.87
Association Energy[b] $\triangle H_{ac}$ (kcal/mol)					
				−12.81	−19.42
Relative Free Energy in the Gas Phase (kcal/mol)					
	0	14.16[c]		−2.31[d]	5.18[d]
Semiempirical Solvation Free Energy (kcal/mol)					
PM3 SM4 (cyclohexane)	−6.19	−6.37	−1.10	−5.78	−5.43
Relative Free Energy in Solution (Solvent=cyclohexane) (kcal/mol)					
	0	13.98[c]		−0.80[d]	7.04[d]

[a] Counterpoise correction has been applied in calculating $\triangle H_{ac}$ and $\triangle G$. [b] $\triangle H_{ac} = H$(complex) − H(2AP or 2PI) − H(acetic acid) − $\triangle E_{cp}$(BSSE). [c] Relative to free 2AP. [d] Relative to free 2AP and acetic acid.

TABLE 2: Critical Bond Distances (in Å) of the 2AP/Acetic Acid, TS, and 2PI/Acetic Acid Calculated by Various Methods in the S_0 State

bond	normal	TS	tautomer
N_1-C_2	1.352[a]	1.379	1.387
	(1.352)[b]	(1.377)	(1.387)
	[1.349][c]	[1.370]	[1.383]
C_2-N_3	1.360	1.318	1.312
	(1.359)	(1.317)	(1.308)
	[1.376]	[1.321]	[1.311]
N_3-H_4	1.020	1.323	1.537
	(1.024)	(1.296)	(1.543)
	[1.019]	[1.262]	[1.593]
H_4-O_5	1.897	1.178	1.059
	(1.882)	(1.199)	(1.055)
	[1.964]	[1.217]	[1.032]
O_5-C_6	1.220	1.293	1.310
	(1.224)	(1.287)	(1.309)
	[1.224]	[1.285]	[1.313]
C_6-O_7	1.320	1.248	1.236
	(1.322)	(1.249)	(1.233)
	[1.328]	[1.252]	[1.233]
O_7-H_8	1.010	1.645	1.749
	(1.019)	(1.598)	(1.731)
	[1.004]	[1.550]	[1.748]
H_8-N_1	1.675	1.055	1.038
	(1.682)	(1.064)	(1.040)
	[1.724]	[1.073]	[1.036]

[a] The numbers are obtained by B3LYP/6-31+G(d′,p′) method. [b] The numbers in the parenthesis () are obtained by B3LYP/6-31G(d′,p′) method. [c] The numbers in the parenthesis [] are obtained by MP2/6-31G(d′,p′) method.

Figure 2. Geometry optimized structures (B3LYP/6-31+G(d′,p′) level) of 2AP/acetic acid, TS and 2PI/acetic acid complexes at the ground electronic states.

well with the concept of conjugated dual hydrogen bonding effect,[13] in which the bond distances relevant to the π-electron delocalization are subject to change. As shown in Table 2, the optimized geometries for both 2AP/acetic and 2PI/acetic complexes, to a certain extent, are affected by the size of the basis sets applied, particularly for those bond distances associated with hydrogen bonds. For example, the B3LYP/6-31+G(d′, p′) method reveals longer H(4)−O(5) ($\Delta r \sim 0.015$ Å, Δr is defined as the difference in bond distance between two applied methods) and shorter H(8)−N(1) ($\Delta r \sim 0.007$ Å) HB distances than those calculated at the level of B3LYP/6-31G(d′,p′) for the 2AP/acetic acid complex, whereas opposite effects on the HB distances (N(3)−H(4), O(7)−H(8)) were found for the case of the 2PI/acetic acid complex. The results indicate the sensible effect upon incorporating diffuse functions on the HB association. Because diffuse functions are large-size versions of s- and p-type
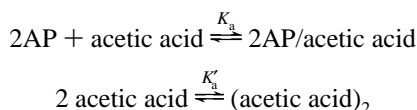
functions, systems such as lone pair electrons in the proton accepting sites, in which the electrons are relatively far from the nucleus, should be affected most significantly. In comparison, the HB distances calculated at the MP2/6-31G(d′,p′) level are all shorter than those calculated by DFT methods. Despite the variation in quantity, relative increments (or decrements) of the crucial bond distances upon complexation listed in Table 2 show a similar trend for all three methods.

Double Proton Transfer in 2-Aminopyridine

J. Phys. Chem. A, Vol. 107, No. 18, 2003 **3247**
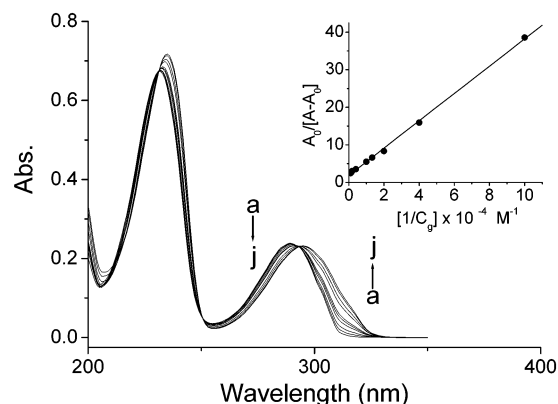
Figure 3. Absorption spectra of 2AP (5.0×10^{-4} M in cyclohexane) as a function of free acetic acid concentration (C_g^0) of a. 0, b. 1.0×10^{-5}, c. 2.5×10^{-5}, d. 5.0×10^{-5}, e. 7.5×10^{-5}, f. 1.0×10^{-4}, g. 2.5×10^{-4}, h. 5.0×10^{-4}, i. 7.5×10^{-4}, j. 1.0×10^{-3} M. Insert: The plot of ($A_0/A - A_0$) at 305 nm as a function of ($1/C_g$) in curves b–j and a best least-squares fitting curve using eq 1.

At the B3LYP/6-31+G(d′,p′) level of theory, the enthalpy and free energy of the HB association, ΔH_{ac} and ΔG, were estimated to be −12.81 and −2.31 kcal/mol, respectively (see Table 1). Experimentally, thermodynamics of the 2AP/acetic acid formation have been studied via the UV−vis absorption titration in isooctane.[24] However, because the association constant of 1.2×10^3 M^{-1} (298 K) deduced in isooctane[24] is relatively small, care has to be taken to consider the competing self-dimerization of acetic acid. In this study, we have carefully performed the UV−vis titration in cyclohexane and derived the thermodynamic parameters on the basis of the competitive equilibrium expressed as

$$2\text{AP} + \text{acetic acid} \underset{}{\overset{K_a}{\rightleftharpoons}} 2\text{AP/acetic acid}$$

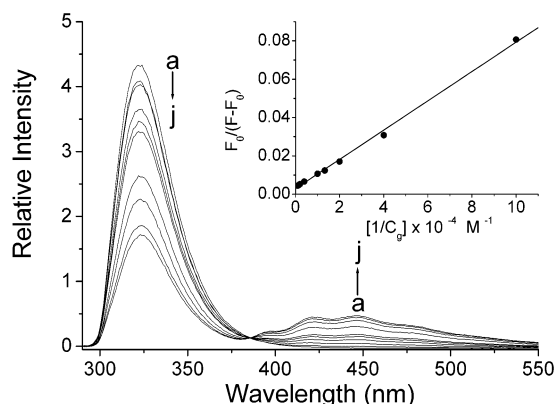$$2 \text{ acetic acid} \underset{}{\overset{K_a'}{\rightleftharpoons}} (\text{acetic acid})_2$$

Based on the negligible consumption of acetic acid upon forming the 2AP/acetic acid complex, the concentration of the free acid, C_g, can be deduced independently by the self-association equation of acetic acid; namely

$$C_g = C_g^0 - \left[\frac{(4K_a'C_g^0 + 1) - \sqrt{8K_a'C_g^0 + 1}}{4K_a'}\right]$$

where C_g^0 is the initially prepared acetic acid concentration. The self-association constant K_a' of acetic acid has been reported to be 3.7×10^4 M^{-1} in *n*-heptane,[45] which was used in the case of cyclohexane because of their similar solvent polarity. Accordingly, the relationship between the measured absorbance as a function of C_g can be expressed by

$$\frac{A_0}{A - A_0} = \frac{\epsilon_M}{\epsilon_M - \epsilon_C}\left(\frac{1}{K_a C_g} + 1\right) \tag{1}$$

where ϵ_M and ϵ_C in eq 1 denote molar extinction coefficients of 2AP monomer and the hydrogen-bonded complex respectively at a specific wavelength. A straight-line plot of ($A_0/A - A_0$) as a function of ($1/C_g$) at a selected wavelength of 290 nm (see Figure 3) supports the validity of the assumption of a 1:1 2AP/acetic acid complex formation. Consequently, a best linear least-squares fit using eq 1 deduces K_a to be $(4.5 \pm 0.3) \times 10^3$ M^{-1} ($\Delta G° = -4.98$ kcal/mol) at 298 K. Temperature-dependent

Figure 4. Fluorescence spectra of 2AP (5.0×10^{-4} M in cyclohexane) as a function of the acetic acid concentration (C_g^0) of a. 0, b. 1.0×10^{-5}, c. 2.5×10^{-5}, d. 5.0×10^{-5}, e. 7.5×10^{-5}, f. 1.0×10^{-4}, g. 2.5×10^{-4}, h. 5.0×10^{-4}, i. 7.5×10^{-4}, j. 1.0×10^{-3} M. Insert: The plot of ($F_0/F - F_0$) at 420 nm as a function of ($1/C_g$) in curves b–j and a best least-squares fitting curve using eq 2.

titration experiments were also performed at 7−40 °C, and ΔH_{ac} was deduced to be −7.8 kcal/mol.

The association constant can also be obtained from the free acetic acid concentration and the measured emission intensity at a selected wavelength expressed in eq 2:

$$\frac{F_0}{F - F_0} = \frac{\Phi_M \epsilon_M}{(\Phi_p \epsilon_p - \Phi_M \epsilon_M)}\left(\frac{1}{K_a C_g} + 1\right) \tag{2}$$

where F_0 and F denote the measured fluorescence intensity prior to and after adding acetic acid. Φ_M and Φ_p are fluorescence quantum yields of the monomer and complex, respectively.[9] The fluorescence titration spectra as well as the plot of $F_0/(F - F_0)$ versus $1/C_g$ are depicted in Figure 4, in which the linear behavior of the plot reconfirms the 1:1 complex formation. A K_a value of $(4.8 \pm 0.2) \times 10^3$ M^{-1} was extracted from a best linear least-squares fit, which within experimental error is consistent with that deduced from the absorption titration study.

In comparison to the experimental data of $\Delta G° \sim -5.0$ kcal/mol, the B3LYP/6-31G+(d′,p′) approach underestimates the strength of the complexation reaction. Incorporating the solvation free energy via the PM3-SM4 solvation model renders a more endergonic value of −0.80 kcal/mol. This may not be surprising because the solvation model is based on the continuum dielectric perturbation and may not accurately describe the 2AP/acetic acid HB system in solution. Another possibility for the discrepancy may be a result of the concentration effect. The intermolecular forces and the solvation effects usually make the free energy different in solution than in the gas-phase, and the extent depends on the concentration and the type of the solvent. The calculated enthalpy and entropy in the DFT approach is for the ideal gas in the standard state, i.e., 1 atm., which is very different from the experimental concentration of $10^{-5}-10^{-3}$ M. In addition, the entropy loss in solution upon complexation is not as important as that in the gas phase. Thus, the free energy of complexation is expected to be more negative in solution, consistent with our current results.

In the ground state, the energy barrier for the 2AP(monomer) → 2PI (monomer) proton (hydrogen atom)[46] transfer tautomerism was estimated to be as large as 48.4 kcal/mol at the B3LYP/6-31+G(d′,p′) level. The result can be rationalized by a four-member-ring conformation between hydrogen donor (pyridinic nitrogen) and acceptor (amino proton) sites in 2AP so that the intramolecular proton (or hydrogen atom[45]) transfer

3248 *J. Phys. Chem. A, Vol. 107, No. 18, 2003*

Hung et al.

TABLE 3: Proton-Transfer Energetics (kcal/mol) in S_0, $S_{\pi\pi^*}$ States at Various Levels of Theory[a,b]

	$\Delta E_1^{\neq}$	E_{int}	$\Delta E_2^{\neq}$	E_{rxn}
S_o State				
HF/6-31G(d′, p′)	12.74	NA	17.10	11.06
MP2/6-31G(d′, p′)//HF/6-31G(d′, p′)	9.36	NA	12.83	11.99
MP2/6-31G(d′, p′)	NA	NA	12.93	11.33
B3LYP/6-31G(d′, p′)	NA	NA	8.63	7.98
B3LYP/6-31+G(d′, p′)	NA	NA	8.17	7.77
$S_{\pi\pi^*}$ State				
CIS/6-31G(d′, p′)	8.48	7.63	7.67	−4.91
TD-B3LYP/6-31+G(d′, p′)// CIS/6-31G(d′, p′)	0.33	−2.29	−2.07	−7.45
CIS/6-31+G(d′, p′)	9.48	8.46	8.67	−4.20
CIS/6-31+G(d′, p′) w/ZPE	6.09	7.12	5.68	−3.97
TD-B3LYP/6-31+G(d′, p′)// CIS/6-31+G(d′, p′)	−0.29	−3.32	−3.62	−8.35
TD-B3LYP/6-31+G(d′, p′) w/ZPE	−3.69	−4.66	−6.60	−8.12

[a] The energy listed is relative to 2AP/acetic acid, of which the total energy is arbitrarily treated as zero. The zero-point and thermal energies are not included. [b] $\Delta E^{\neq}$, energy barrier; E_{int}, energy of the intermediate; E_{rxn}, energy of the 2AP/acetic acid → 2PI/acetic acid proton-transfer reaction.

reaction is expected to be associated with enormously high strain energy. Upon forming the 2AP/acetic acid complex, the proton-transfer energy barrier is drastically reduced through the catalysis of acetic acid. Table 3 shows the proton-transfer energetics in the ground state at various levels of theory, in which the energy listed is relative to that of the 2AP/acetic acid. All calculations predicted the proton-transfer tautomer, i.e., 2PI/acetic acid, to be higher in energy than the normal form by 8−12 kcal/mol. DFT reduces the energy difference in comparison to Hartree−Fock and MP2 methods. The incorporation of diffuse functions has a negligible effect on the reaction thermodynamics.

As shown in Table 3, two transition states were resolved at either the Hartree−Fock (6-31G(d′,p′) basis set) level or MP2/6-31G(d′,p′) with geometry optimized at the Hartree−Fock level (e.g., 6-31G(d′,p′)). However, applying the electron correlation (MP2 or DFT) in the geometry optimization results in only one transition state. The single transition state may be further supported by the failure to locate an intermediate along the ground-state potential energy surface (PES) among the various methods applied. The calculated classical barrier height of the forward reaction, depending on the levels of methods, ranges from 8 to 17 kcal/mol. With the same basis set, values of the barrier obtained by the B3LYP method are ~8 and ~4 kcal/mol lower than those predicted at the Hartree−Fock and MP2 levels, respectively. This discrepancy is believed to be due to the different ways of treating (or neglecting) the electron correlation. The correlation energy was treated only semiempirically in the hybrid DFT, which is known to underestimate the barrier heights of many types of reactions. The diffuse functions lowered the barrier height only slightly.

The energy barrier of reverse proton transfer (i.e., 2PI/acetic acid → 2AP/acetic acid) was calculated to be 6.04, 1.60, and 0.65 kcal/mol at HF/6-31G(d′,p′), MP2/6-31G(d′,p′), and B3LYP/6-31G(d′,p′) levels, respectively. A similar trend was thus observed in both forward and reverse proton-transfer reactions, in which the Hartree−Fock method overestimates the reaction barrier because of the negligence of the electron correlation. For both MP2 and DFT methods, the calculated barrier is so small that the reaction barrier on the reverse proton-transfer becomes negligible upon addition of the zero-point energy.

In consideration of the ground transition-state (TS) geometry, among the various calculation methods shown in Table 2,

**TABLE 4: pK_a and pK_a^* Values for Various Functional Groups in 2AP and Acetic Acid (ACID)**

	2AP (N(1)H$^+$)	2AP (N(3)H2)	ACID (−O(7)H)	ACID (=O(5)H$^+$)
pK_a	6.86[a]	23.50[b]	4.75[c]	−6.5[c]
pK_a^*	8.95[a]	~ 20.20[d]		

[a] Weisstuch, A.; Testa, A. C. *J. Phys. Chem.* **1968**, *72*, 1982. [b] Harris, M. G.; Stewart, R. *Can. J. Chem.* **1977**, *55*, 3800. [c] Gordon, A. J.; Ford, R. A. *The Chemist's Companion*; John Willey & Son: New York, 1972. [d] Calculated by the Förster cycle.

significant changes of H(8)−N(1) ($\Delta r \sim -0.62$ Å) and O(7)−H(8) ($\Delta r \sim +0.63$ Å) distances were observed in the TS relative to the 2AP/acetic acid complex. Although the shortening of the H(4)−O(5) bond distance ($\Delta r \sim 0.7$ Å) is also significant, the elongation of the N(3)−H(4) distance is relatively smaller ($\Delta r < 0.3$ Å) (see Table 2 and Figure 2). This, in combination with the fact that only one TS was resolved, led us to conclude that the double proton transfer may take place through a concerted, asynchronous pathway in the ground state. At the TS, the carboxylic hydrogen on the acetic acid has already been transferred to the pyridinic nitrogen, whereas the amino hydrogen has just begun to move toward the carbonyl oxygen of acetic acid. Empirically, the hydrogen-bond strength correlates with the pK_a and pK_b of the proton donor and acceptor, respectively, in the ground state. It increases with the acidity of the donor atom and the basicity of the acceptor group.[15a,23,47,48] Accordingly, the HB strength is expected to increase as the sum of pK_a + pK_b decreases. Table 4 summarizes pK_a values of various hydrogen bonding sites for 2AP and acetic acid. Apparently, the value of pK_a (donor) + pK_b (acceptor) ($pK_b = pK_{H_2O} - pK_a$ (protonated acceptor) where K_{H_2O} is the autoprotolysis constant of H_2O) was calculated to be on the order of 2AP(−N(3)−H)/acetic acid (=O) ≫ 2AP(−N(1)-)/acetic acid (−OH). Such an empirical approach predicts a stronger pyridinic nitrogen-carboxylic (−OH) hydrogen-bonding strength, which is also consistent with its calculated shorter bond distance. It is thus reasonable to conclude that the initial stage of reaction involves proton transfer via the carboxylic hydrogen to the pyridinic nitrogen, followed by the proton transfer from the amino hydrogen to the carbonyl oxygen.

3.2. Approaches in the Excited States. With our current computing capacity, the converged complete active space-self-consistent field (CASSCF) calculations with extended basis sets are not practical in dealing with the 2AP/acetic acid system. Alternatively, the CIS method, which has been proven to be a relatively useful method to obtain the approximate wave function and molecular geometry of electronic excited states, was applied in this study. However, the CIS method usually overestimates the energy differences between the excited and ground states as well as the excited-state barriers. Conversely, although the time-dependent DFT method currently cannot perform geometry optimization at the excited states, it has been shown to be able to gain very reliable vertical excitation energies of low-lying excited states.[49] Thus, an attempt at estimating the normal energy gap of absorption has also been made on a vertical excitation in which the excited-state geometry was taken from the ground-state optimized structure. This has been performed using the TD-B3LYP level at B3LYP geometry.

Figure 5 depicts the structures of the two lowest unoccupied and two (CIS level) or three (TD-B3LYP level) highest occupied frontier molecular orbitals mainly involved in the transition of low-lying excited states using either the CIS//HF/6-31+G(d′,p′) or TD-B3LYP//B3LYP/6-31+G(d′,p′) method. Depending on levels of theory, the calculations differ slightly in the nature of

Double Proton Transfer in 2-Aminopyridine

J. Phys. Chem. A, Vol. 107, No. 18, 2003 **3249**
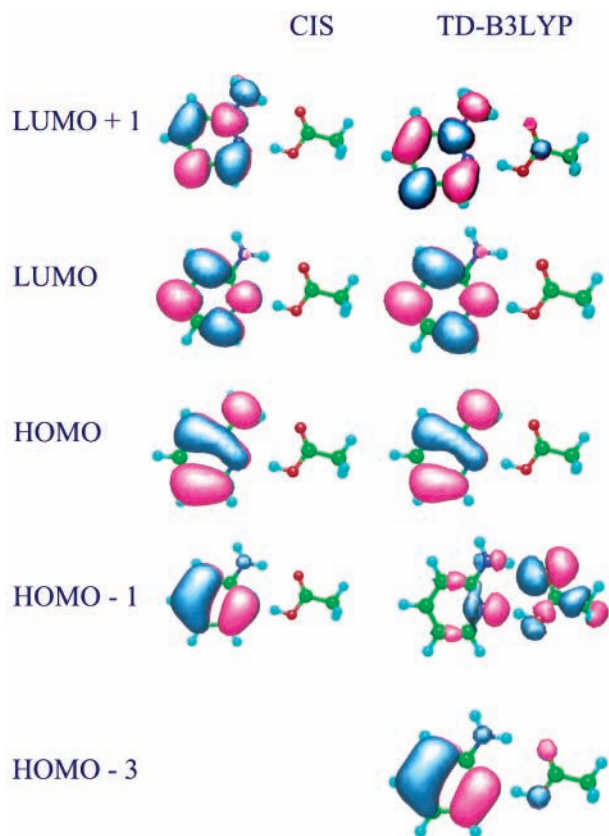
Figure 5. Calculated (CIS//HF/6-31G(d′,p′) and TD-B3LYP//B3LYP/6-31G(d′,p′) methods) frontier molecular orbitals for the 2AP/acetic acid complex.

the molecular orbitals involved in the predominant excitations. For example, the S_1 state has a contribution from HOMO → LUMO, LUMO + 1 in the TD-B3LYP calculations versus HOMO-1, HOMO → LUMO in the CIS computations. However, both methods predicted a similar trend where the S_1 state in the 2AP/acetic acid complex can be well ascribed using an allowed (π-symmetry) → π^* (π-symmetry) transition (see Table 5). With the use of the TD-B3LYP method incorporating the B3LYP/6-31+G(d′,p′) optimized geometry, the vertical excitation energy from the ground-state normal form to the $^1\pi\pi^*$ state was calculated to be 101.2 kcal/mol (35 473 cm^{-1}), which is consistent with the experimentally determined λ_{max} of $S_0 \to S_1$ absorption of ~98.6 kcal/mol (34 482 cm^{-1}) for the first $\pi\pi^*$ singlet excited state (see Figure 3). In addition, the calculated oscillator strength, f, of 0.063 is in agreement with that of 0.065 deduced from the extinction coefficient ϵ of absorption. In consideration of the excitation energetics of the proton-transfer tautomer, a better comparison with spectroscopic (i.e., fluorescence) data would be using the CIS/6-31+G(d′,p′) optimized geometry for the excited state and, alternatively, performing the vertical excitation on the basis of the TD-B3LYP method. The energy gap between $^1\pi\pi^*$ and ground state for the 2PI/acetic acid complex was calculated to be 76.1 kcal/mol (26 610 cm^{-1}), which is consistent with the experimental value of ~75.2 kcal/mol (26 292 cm^{-1}) estimated from the proton-transfer tautomer, i.e., 2PI/acetic acid complex, emission. The calculated oscillator strength of 0.053 (see Table 5) is also on the same magnitude as that of 0.031 deduced experimentally by using $k_r \sim \tilde{v}_0^2 f$ where k_r (2.11 × 10^7 s^{-1}) and $\tilde{v}_0$ (26 292 cm^{-1}) denote radiative decay rate constant and fluorescence energy gap of the proton-transfer tautomer, respectively.

Based on the CIS/6-31+G(d′,p′) level of theory, an enormously high energy barrier of 41.5 kcal/mol was obtained for

the 2AP monomer → 2PI monomer proton-transfer reaction in the first $^1\pi\pi^*$ excited state, albeit the reaction is thermodynamically favorable by 5.3 kcal/mol. Similar to the aforementioned ground-state proton transfer reaction, the high energy barrier resulting from the strain energy can be drastically reduced upon the catalysis of acetic acid. However, unlike the single TS calculated in the ground-state proton-transfer reaction, two transition states specified as TS_1 and TS_2 were resolved at the CIS/6-31+G(d′,p′) level of theory. The 2AP/acetic acid → TS_1 process associates with a classical barrier of 9.48 kcal/mol. Analyses of the TS_1 geometry (see Figure 6 and Table 6) reveal significant proton migration with the N(1)−H(8) distance of 1.180 Å relative to that of 1.848 Å in the normal complex. Conversely, TS_2 is 8.67 kcal/mol higher in energy than the excited normal (i.e., 2AP/acetic acid) species. The geometry of TS_2 shows a nearly complete N(1)−H(8) covalent bonding formation, whereas the migration of the N(3)H(4) proton becomes appreciable, as indicated by the drastic elongation of the N(3)H(4) bonding distance of 0.75 Å from TS_2 (1.141 Å) to the tautomer species (1.897 Å). At the CIS/6-31+G(d′, p′) level of theory, we were also able to locate an intermediate. However, the energy of the intermediate is only 0.21 kcal/mol lower than that of TS_2.

We have made an attempt to locate the proton-transfer reaction pathway in the $^1\pi\pi^*$ electronic state via scanning the PES. Unfortunately, a two-dimensional relaxed scan of the PES in the $^1\pi\pi^*$ configuration is extremely time-consuming and hence is not feasible at this stage. Alternatively, because the change of bond distance at the C=O(5)···H(4)N hydrogen bonding site is slower than that at the COOH(8)···N(1) site, we simply scanned the COOH(8)···N(1) hydrogen-bonding distance by 0.01 Å in each step at the CIS/6-31G(d′,p′) level. Simultaneously, we allowed a full optimization on the remaining bond angles and distances in the $^1\pi\pi^*$ configuration. As shown in Figure 7, although TS_1 was resolved through this profile method, we were not able to locate TS_2 and hence an intermediate. The difference between the direct optimization (two TS) and the profile method (one TS) clearly indicates a very shallow PES nearby the intermediate and TS_2. This viewpoint will be further discussed in the following sections. We also performed an alternative attempt, in which the PES was scanned through the −NH(4)- - -O(5)=C− reaction coordinate. The result renders a much higher barrier than that through the COOH(8)- - -N(1)− pathway, supporting the asynchronous type of excited-state double proton transfer, in which the hydrogen moves earlier along the COOH(8)···N(1) hydrogen-bonding site.

It should be noted that the CIS method only includes a small fraction of the correlation energy.[27] Higher-level correlation methods might reduce the energy barrier. We thus performed the energy profile calculations using the TD-B3LYP method on reactant and TS geometries that were initially optimized at the CIS/6-31G(d′,p′) level. Although the results at the TD-B3LYP/CIS/6-31+G(d′,p′)//CIS/6-31G(d′,p′) level revealed the existence of two transition states, the classical barrier of the 2PA/acetic acid → TS_1 reaction has been reduced to 0.33 kcal/mol. However, the results incorporating TD-B3LYP for energetic calculation are sensitive to the choice of basis sets to optimize the geometry. For example, by applying additional diffuse functions for the basis set (i.e., 6-31+G(d′,p′)), both TS_1 and TS_2 disappear. In the previous section, it has been demonstrated that calculations of the energy gap between the ground and first excited states seem reliable for both normal and tautomer forms at the stationary points. The validity of this

TABLE 5: Low-Lying Singlet Electronic Transitions ($S_{\pi\pi*}$) of 2AP/Acetic Acid and 2PI/Acetic Acid Calculated via TD-B3LYP and CIS Methods

methods	dominant configurations[a]	vertical excitation energy (kcal/mol)	oscillator strength (*f*)
	2AP/Acetic Acid		
TD-B3LYP//B3LYP/6-31G(d′, p′)	H → L; H → L+1	104.7	0.0589
TD-B3LYP//B3LYP/6-31+G(d′, p′)		101.2	0.0628
CIS//HF/6-31G(d′, p′)	H−1 → L; H → L	135.6	0.1567
	2PI/Acetic Acid[b]		
TD-B3LYP/6-31G(d′, p′)	H → L	77.9	0.0511
TD-B3LYP/6-31+G(d′, p′)		76.1	0.0533
CIS/6-31+G(d′, p′)	H → L; H → L+1	122.9	0.0330

^{a} H, HOMO; L, LUMO. ^{b} At the CIS/6-31+G(d′,p′) optimized excited-state geometry.
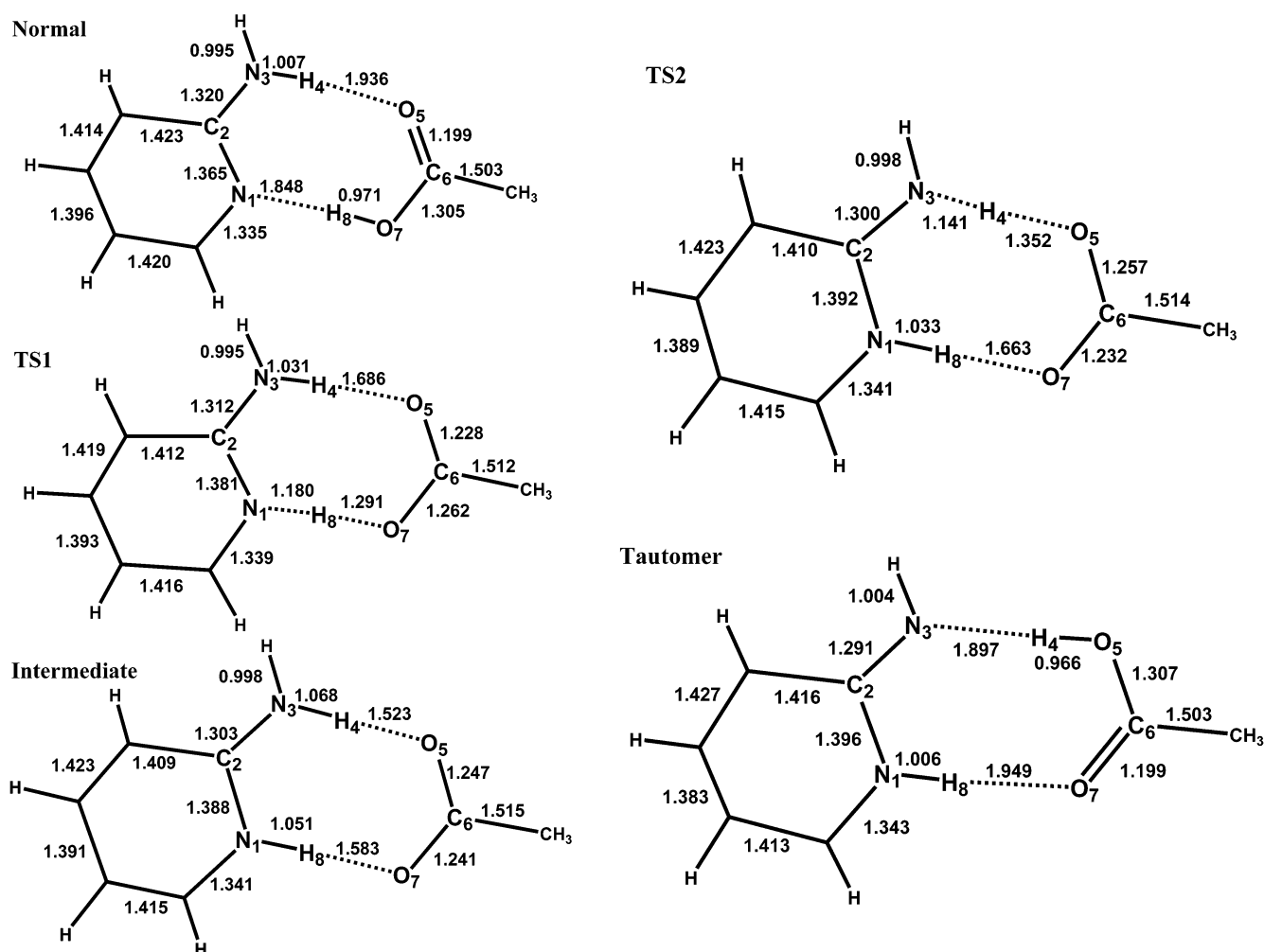
Figure 6. Calculated stationary point geometry at CIS/6-31+G(d′,p′) level for normal, TS and proton-transfer tautomer of the 2AP/acetic acid complex in the $S_{\pi\pi*}$ state.

approach is believed to be mainly due to the relative insensitivity upon the geometry variation at the energy minimum. In contrast, considering the TS to be much more dynamic, a small adjustment of the geometry might lead to qualitatively different energetics. Because DFT and CIS are expected to associate with different TS structures, the approach of TS energetics incorporating TD-B3LYP//CIS methods might be subject to a great deal of uncertainty.

Among various levels of theoretical approaches, only by using the CIS level can one resolve the intermediate. The potential energy well of the intermediate seems to be very shallow, in which the second energy barrier was estimated to be as small as 0.21 kcal/mol based on the CIS/6-31G+(d′,p′) level of theory. If one incorporates the zero-point energy (ZPE), the second step

might proceed through a negligible barrier. Furthermore, the intermediate could not be trapped upon applying the electron correlation such as the CIS-MP2 level on the CIS optimized geometries of the intermediate and TS. One may consider that the CIS-MP2 level might not be appropriate in dealing with PES either because the optimized geometry could be quite different or the unbalanced treatment of correlation energy in the excited state at different geometries. Apparently, when using CIS-MP2 or TD-DFT with diffuse functions, the energy of TS$_2$ is actually lower than that of the intermediate. Consequently, both TS$_2$ and the intermediate cannot be trapped, further supporting a rather small energy barrier for the second-step proton-transfer process.

Double Proton Transfer in 2-Aminopyridine

J. Phys. Chem. A, Vol. 107, No. 18, 2003 **3251**

TABLE 6: Critical Bond Distance (Å) of 2AP/Acetic Acid Normal, TS$_1$, Intermediate, TS$_2$, and Proton-Transfer Tautomer Calculated by CIS/6-31+G(d′,p′) and CIS/6-31G(d′,p′) in S$_{\pi\pi*}$ States^a

bond	normal	TS$_1$	intermediate	TS$_2$	tautomer
N$_1$–C$_2$	1.365	1.381	1.388	1.392	1.396
	(1.375)	(1.386)	(1.391)	(1.393)	(1.399)
C$_2$–N$_3$	1.320	1.312	1.303	1.300	1.291
	(1.323)	(1.313)	(1.305)	(1.302)	(1.291)
N$_3$–H$_4$	1.007	1.031	1.068	1.141	1.897
	(1.005)	(1.033)	(1.082)	(1.123)	(1.870)
H$_4$–O$_5$	1.936	1.686	1.523	1.352	0.966
	(1.929)	(1.667)	(1.476)	(1.383)	(0.967)
O$_5$–C$_6$	1.199	1.228	1.247	1.257	1.307
	(1.198)	(1.227)	(1.247)	(1.253)	(1.306)
C$_6$–O$_7$	1.305	1.262	1.241	1.232	1.199
	(1.302)	(1.259)	(1.237)	(1.232)	(1.197)
O$_7$–H$_8$	0.971	1.291	1.583	1.663	1.949
	(0.975)	(1.295)	(1.583)	(1.627)	(1.948)
H$_8$–N$_1$	1.848	1.180	1.051	1.033	1.006
	(1.802)	(1.175)	(1.048)	(1.039)	(1.005)

^{a} (), CIS/6-31G(d′,p′).

Excited State One-Dimensional Scan of 2AP/acetic acid
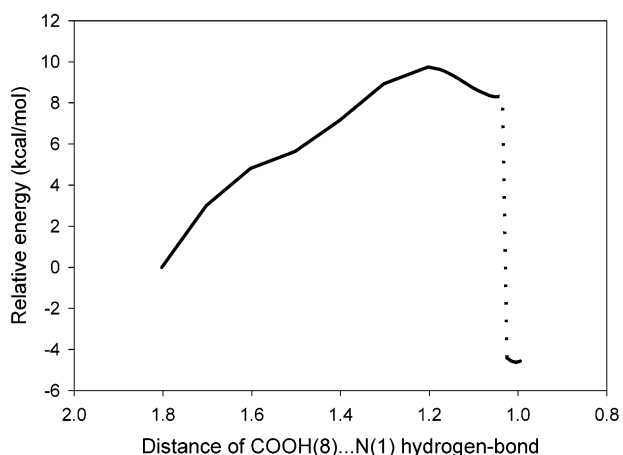
Figure 7. Calculated potential energy surface (CIS/6-31G(d′,p′)) along the proton-transfer reaction in the first excited singlet state, in which the COOH(8)···N(1) hydrogen-bonding distance was scanned by 0.01 Å in each step. The rest of bond angles and distances were fully optimized.

4. Discussion

4.1. Factors Affecting the Association. The association constant of the 2AP/acetic HB formation ($\sim$4.5 × 10^3 M^{-1}) is apparently smaller than that of the 7AI/acetic acid HB complex ($\sim$2.2 × 10^4 M^{-1})[13b] in cyclohexane. Factors such as the steric effect may play a key role to fine-tune the stability of various 2AP hydrogen-bonded species. At the B3LYP/6-31+G(d′, p′) level of theory, the H(4)–N(3)–C(2) plane was calculated to be 16.3 ° with respect to the pyridine plane in a geometry optimized 2AP monomer form, whereas it was calculated to be 9.9° for the case of the 2AP/acetic acid complex. The result indicates that a sterically hindered rotation of the N(1)–H bond toward a favorable configuration is necessary prior to the complexation, of which the associated endothermic energy compensates for the gain of the stabilization because of the dual hydrogen-bonding formation. We further truncated the 2AP/acetic acid complex by removing the dual hydrogen bond but holding the structures unchanged. The results indicate that the truncated 2AP is $\sim$1.5 kcal/mol higher in energy than that of the geometry optimized 2AP monomer. Because a torsional angle of 9.9° is obtained when the strain energy (an endothermic

process) plus hydrogen-bonding energy (an exothermic process) reach a minimum value upon complexation, the sacrifice of certain hydrogen-bonding energy is necessary to avoid increasing the strain energy toward planarity. Accordingly, a larger steric effect was even expected in the case of 2AP dimer in which both N(3)–H(4) bonds of two 2AP monomers must be adjusted prior to the dimerization. This consequence explains the calculated ΔH_{ac} of −6.8 kcal/mol for the 2AP dimer at the B3LYP/6-31+G(d′, p′) level of theory (not shown here), which is less exothermic than that of −11.5 kcal/mol calculated for the 7AI dimer[13b] in which the planar geometry of 7AI facilitates the dual HB formation

4.2. ESDPT Mechanism, Theoretical vs Experimental Approaches. As mentioned earlier, in the picosecond dynamic approach, Ishikawa et al.[26] were able to extract a 360 nm transient cationic emission band. The results, in combination with the deuterium isotope-dependent reaction dynamics, led them to conclude a stepwise acetic acid-catalyzed proton-transfer reaction. The first step incorporating a COOH(8) → N(1) proton transfer is too fast to be resolved, forming a zwitterionic type of intermediate, followed by the second proton-transfer step from the amino proton back to the carboxylate ion.

Theoretical approaches at the CIS/6-31+G(d′,p′) level of theory resolved two transition states during ESDPT in the 2AP/acetic acid system. The first TS incorporates the migration of the carboxylic proton to the pyridinic nitrogen, whereas the motion of the amino proton is obviously involved in the second TS. Regarding the kinetic isotope effect (KIE) for the first step, we have also calculated the ZPE differences between the protonated and deuterated reactions. The ZPE-corrected barrier of the deuterated reaction is 1.02 kcal/mol higher at the CIS/6-31+G(d′,p′) level. Thus, in thermal equilibrium, this would translate to a approximately 5.5 times slower rate constant at 300 K, which is somewhat higher than the experimental report of 1.4.[26] Because there are perhaps significant populations at higher vibronic energy levels in the excited state, the KIE may not be as significant as that derived simply from the ZPE difference in the theoretical approach.

The stepwise proton transfer reaction in the 2AP/acetic acid system may also be qualitatively rationalized by the significant difference in the hydrogen bonding strength. Table 4 lists pK_a* values for the protonated pyridinic nitrogen and amino proton in the excited state. Because acetic acid is not incorporated in the excitation chromophore, its ground-state pK_a values of +4.75 and −6.5 were applied to carboxylic proton (−COOH(8)) and C=O(5)H$^+$ sites, respectively. According to Table 4, the sum of pK_a* + pK_b* of 9.8 for the −COOH(8)- - -N(1) pair is significantly smaller than that of $\sim$40 for the −N(3)H- - -O(5)=C− pair, indicating a stronger −COOH(8)- - -N(1) hydrogen bonding strength in the excited state. The decrease in the hydrogen bonding distance is expected to correspondingly reduce the barrier height upon executing the proton-transfer reaction.

The stepwise ESDPT mechanism for the 2AP/acetic acid system seems to be consistent with the experimental approaches. Being the same with regards a two-step mechanism, there however exist important differences between the theoretical and experimental approaches. The barrier for the first proton-transfer step seems to be significantly larger than that for the second step. For example, calculations on the CIS level estimated the first barrier to be 9.48 kcal/mol (6.09 kcal/mol after adding the ZPE), whereas the second-step proton transfer is negligibly small as indicated by the failure to trap the intermediate. Accordingly, although both experimental and theoretical approaches are in

agreement on the two-step mechanism, they reveal certain discrepancies in terms of the kinetic expression. Experimental results conclude a fast, nonresolvable (≪5 ps) first step, followed by a slow, resolvable (∼5 ps) second step, whereas the theoretical approaches seem to favor the slow first-step with fast second-step rates of the ESDPT reaction.

Is it possible to rationalize the experimental results alternatively from the theoretical basis? To answer this question, we have thus made an attempt to deduce the reaction kinetics based on the theoretical approach. Scheme 1 qualitatively depicts the PES of acetic acid-catalyzed ESDPT in 2AP, in which N^*, I^* and T^* denote normal form, intermediate, and tautomer, respectively, in the excited state. In accordance with the theoretical results, the reaction incorporates a slow first-step and fast second-step proton-transfer process. Both steady state and dynamic approaches indicate that the ESDPT reaction in the 2AP/acetic acid system is exergonic and irreversible. Therefore, the formation and relaxation dynamics for N^*, I^*, and T^* can thus be expressed as

$$\frac{d[N^*]}{dt} = -k_{pt_1}[N^*] \tag{3}$$

$$\frac{d[I^*]}{dt} = k_{pt_1}[N^*] - k_{pt_2}[I^*] \tag{4}$$

$$\frac{d[T^*]}{dt} = k_{pt_2}[I^*] - k_T[T^*] \tag{5}$$

where k_T is the observed decay rate of the tautomer emission, k_{pt_1} and k_{pt_2} denote the rate constants of first- and second- step proton-transfer reaction, respectively. Note the nonproton-transfer decay rate of $[N^*]$ is relatively small and has been neglected in (3). Because the barrier of the first proton-transfer step is higher in energy than that of the second one, it is reasonable to assume k_{pt_2} to be $\gg k_{pt_1}$. Assuming the electronic excitation with infinitesimal pulse duration, $[N^*]$, $[I^*]$, and $[T^*]$ are derived to be

$$[N^*] = [N^*]_0 e^{-k_{pt1}t} \tag{6}$$

$$[I^*] = \frac{k_{pt_1}}{k_{pt_2}}[N^*]_0 e^{-k_{pt1}t} \tag{7}$$

$$[T^*] = \frac{k_{pt_1}}{k_T - k_{pt_1}} e^{-k_{pt1}t} - \frac{k_{pt_1}}{k_T - k_{pt_1}} e^{-k_T t} \tag{8}$$

where $[N^*]_0$ is the instant population of the N^* species at $t = 0$. Apparently, both reactant and intermediate undergo identical decay dynamics of k_{pt_1}. In the case of the intermediate $[I^*]$, the observed decay dynamics actually corresponds to the rate of the first proton-transfer reaction. The reason where k_{pt_1} appears in the decay expression of $[I^*]$ is simply due to the much faster k_{pt_2} which is expressed as an irresolvable rise component. Conversely, if $k_{pt_1} > k_T$, which is generally the case, a rise dynamics with k_{pt_1} was expected for the tautomer species. Thus, the decay dynamics of the intermediate corresponds to the rise dynamics of the tautomer emission, consistent with the experimental results. It thus seems unnecessary to incorporate fast first step proton-transfer dynamics for interpreting the fast rise component of the cationic intermediate.[26]

Nevertheless, cautions still have to be taken from the proposed mechanism above. First, according to Scheme 1, $[I^*]$ might be too small an amount to be detectable because of $k_{pt_2} \gg k_{pt1}$ in

SCHEME 1
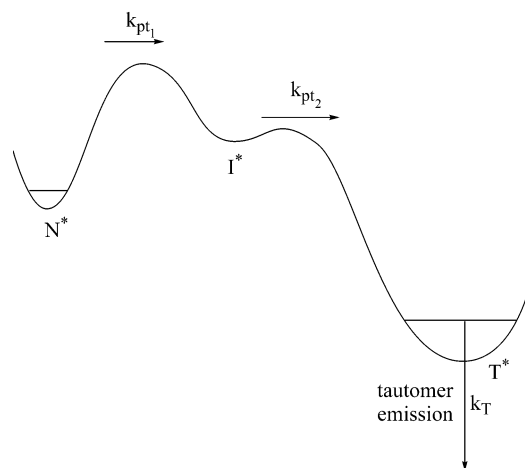
eq 7. Second, the dynamics of normal emission has to be rationalized, which should consist of dual components, namely, the uncomplexed 2AP and 2AP/acetic acid complex, and the decay of the normal emission of the 2AP/acetic acid complex dominated by the proton-transfer reaction. According to the two-step mechanism depicted in Scheme 1 and eq 6, a decay component of 5 ps ought to be resolved. This prediction seems contradictory to the observed relaxation dynamics monitored at 325 nm (see Figure 6a in ref 26), in which an irresolvable rise component was obtained, followed by a long-lived decay component ascribed to the free 2AP normal emission.[26] On one hand, the result may simply indicate that the originally prepared 2AP/acetic acid concentration was relatively small so that the 5 ps component attributed to the fast decay of the 2AP/acetic acid emission might be buried inside the free 2AP emission. However, the corresponding steady-state fluorescence titration spectra (see Figure 2 in ref 26) indicated that more than 15% of 2AP/acetic acid should exist in the ground-state equilibrium. Therefore, unless the radiative lifetime of the 2AP/acetic acid system is much smaller than that of the free 2AP, this interpretation does not seem quite possible. On the other hand, owing to the dual hydrogen bonding effect, if the spectra could be resolved from the time-dependent spectral evolution, its emission maximum should be red shifted with respect to the steady-state resolved normal emission of free 2AP. In an extreme case, the normal hydrogen-bonded complex emission might even overlap with that of the cationic intermediate significantly. Certainly, without further experimental details one should not speculate too much on this issue.

5. Conclusion

In conclusion, theoretical approaches to the ground- and excited-state double proton transfer in the 2-aminopyridine (2AP)/acetic acid dual HB system have been performed. Comparisons have been made between thermodynamic parameters deduced from the theoretical approach and those extracted by absorption and fluorescence titration studies. The first excited singlet state of the 2AP/acetic acid system possesses a $\pi\pi^*$ configuration, in which two transition-state geometries were resolved for the 2AP/acetic acid → 2(*1H*)-pyridinimine/acetic acid double proton transfer at the CIS/6-31+G(d′, p′) level. The sequence of the asynchronous double proton-transfer correlates well with the hydrogen-bonding strength. Although both experimental[26] and theoretical approaches concluded a two-step ESDPT process, differences have been addressed on the rate-determining step. However, because the cationic-like intermedi-

Double Proton Transfer in 2-Aminopyridine

J. Phys. Chem. A, Vol. 107, No. 18, 2003 **3253**

ate may be very sensitive to the solvent-polarity perturbation, the theoretical approach to the excited state, in which the solvent interaction is neglected, may stand in far comparison with respect to the experimental results. Solvent polarization and/or dynamics have been reported to play crucial roles in ESDPT dynamics for the case of 7-azaindole types of HB complexes.[8−13] A similar trend would be expected in the case of 2AP HB complexes. Last but not least, it is also plausible that theoretical approaches incorporating higher levels of electron correlation are necessary to rationalize the experimental results. Nevertheless, this study renders a theoretical basis for the host/guest types of ESDP systems possessing unequivalent dual hydrogen bonds. Further femtosecond dynamics as well as solvent/temperature-dependent studies, in combination with higher-level theoretically approaches (e.g., CASSCF calculations[50]), are required to unveil more insight into the mechanism of ESDPT in the 2AP/acetic acid system.

References and Notes

(1) For review, see: (a) Kasha, M. *J. Chem. Soc., Faraday Trans. 2* **1986**, *82*, 2379. (b) Waluk, J. *Conformational analysis of Molecules in Excited States*; Wiley-VCH: New York, 2000. (c) Chou, P. T. *J. Chin. Chem. Soc.* **2001**, *48*, 651.

(2) Taylor, C. A.; El-Bayoumi, M. A.; Kasha, M. *Proc. Natl. Acad. Sci. U.S.A.* **1969**, *63*, 253.

(3) Ingham, K. C.; El-Bayoumi, M. A. *J. Am. Chem. Soc.* **1974**, *96*, 1674.

(4) Takeuchi, S.; Tahara, T. *J. Phys. Chem. A* **1998**, *102*, 7740.

(5) (a) Chachisvilis, M.; Fiebig, T.; Douhal, A.; Zewail, A. H. *J. Phys. Chem. A* **1998**, *102*, 669. (b) Fiebig, T.; Chachisvilis, M.; Manger, M.; Zewail, A. H.; Douhal, A.; Garcia-Ochoa, I.; de La Hoz Ayuso, A. *J. Phys. Chem. A* **1999**, *103*, 7419.

(6) Douhal, A.; Guallar, V.; Moreno, M.; Lluch, J.-M. *Chem. Phys. Lett.* **1996**, *256*, 370.

(7) (a) Catalán, J.; Carles del Valle, J.; Kasha, M. *Proc. Natl. Acad. Sci. U.S.A.*, **1999**, *96*, 8338. (b) Catalán, J.; Kasha, M. *J. Phys. Chem. A* **2000**, *104*, 10812.

(8) (a) Chapman, C. F.; Maroncelli, M. *J. Phys. Chem.* **1992**, *96*, 8430. (b) Mente, S.; Maroncelli, M. *J. Phys. Chem. A* **1998**, *102*, 3860.

(9) Smirnov, A. V.; English, D. S.; Rich, R. L.; Lane, J.; Teyton, L.; Schwabacher, A. W.; Luo, S.; Thornburg, R. W.; Petrich, J. W. *J. Phys. Chem. B* **1997**, *101*, 2758 and references therein.

(10) Chaban, G. M.; Gordon, M. S. *J. Phys. Chem. A* **1999**, *103*, 185.

(11) Smedarchina, Z.; Siebrand, W.; Fernández-Ramos, A.; Gorb, L.; Leszczynski, J. *J. Chem. Phys.* **2000**, *112*, 566.

(12) Kyrychenko, A.; Stepanenko, Y.; Waluk, J. *J. Phys. Chem. A* **2000**, *104*, 9542.

(13) (a) Chou, P. T.; Wei, C. Y.; Chang, C. P.; Chiu, C. H. *J. Am. Chem. Soc.* **1995**, *117*, 7259. (b) Chou, P. T.; Wei, C. Y.; Chang, C. P.; Kuo, M. S. *J. Phys. Chem.* **1995**, *99*, 11994. (c) Chou, P. T.; Wei, C. Y.; Wu, G. R.; Chen, W. C. *J. Am. Chem. Soc.* **1999**, *121*, 12186. (d) Chou, P. T.; Wu, G. R.; Wei, C. Y.; Cheng, C. C.; Chang, C. P.; Hung, F. T. *J. Phys. Chem. B* **1999**, *103*, 10042. (e) Chou, P. T.; Liao, J. H.; Wei, C. Y.; Yang, C. Y.; Yu, W. S.; Chou, Y. H. *J. Am. Chem. Soc.* **2000**, *122*, 986.

(14) Song, P. S.; Sun, M.; Koziolowa, A.; Koziol, J. *J. Am. Chem. Soc.* **1974**, *96*, 4319.

(15) (a) Chou, P. T.; Wei, C. Y.; Wang, C. C.; Hung, F. T.; Chang, C. P. *J. Phys. Chem. A* **1999**, *103*, 1939 and reference therein. (b) Wei, C. Y.; Yu, W. S.; Chou, P. T.; Hung, F. T.; Chang, C. P.; Lin, T. C. *J. Phys. Chem. B* **1998**, *102*, 1053.

(16) (a) Herbich, J.; Hung, C. Y.; Thummel, R. P.; Waluk, J. *J. Am. Chem. Soc.* **1996**, *118*, 3508. (b) Kyrychenko, A.; Herbich, J.; Wu, F.; Thummel, R. P.; Waluk, J. *J. Am. Chem. Soc.* **2000**, *122*, 2818.

(17) Ríos Rodríguez, M. C.; Mosquera, M.; Rodríguez-Prieto, F. *J. Phys. Chem. A* **2001**, *105*, 10249.

(18) (a) Kyrychenko, A.; Herbich, J.; Izydorzak, M.; Wu, F.; Thummel, R. P.; Waluk, J. *J. Am. Chem. Soc.* **1999**, *121*, 11179. (b) Marks, D.; Zhang, H.; Borowicz, P.; Waluk, J.; Glasbeek, M. *J. Phys. Chem. A* **2000**, *104*, 7167. (c) Kyrychenko, A.; Stepanenko, Y.; Waluk, J. *J. Phys. Chem. A* **2000**, *104*, 9542.

(19) Carles del Valle, J.; Dominguez, E.; Kasha, M. *J. Phys. Chem. A* **1999**, *103*, 2467.

(20) (a) Varela, A. P.; Miguel, M. da G.; Macanita, A. L.; Burrows, H. D.; Becker, R. S. *J. Phys. Chem.* **1995**, *99*, 16093. (b) Dias, A.; Varela, A. P.; Miguel, M. da G.; Macanita, A. L.; Becker, R. S. *J. Phys. Chem.* **1992**, *96*, 10290.

(21) (a) Reyman, D.; Pardo, A.; Poyato, J. M. L. *J. Phys. Chem.* **1994**, *98*, 10408. (b) Reyman, D.; Viñas, M. H.; Poyato, J. M. L.; Pardo, A. *J. Phys. Chem. A* **1997**, *101*, 768. (c) Reyman, D.; Viñas, M. H. *Chem. Phys. Lett.* **1999**, *301*, 551.

(22) (a) Balón, M.; Muñoz, M. A.; Guardado, P.; Carmona, C. *Photochem. Photobiol.* **1996**, *64*, 531. (b) Balón, M.; Carmona, C.; Guardado, P.; Muñoz, M. A. *Photochem. Photobiol.* **1998**, *67*, 414. (c) Carmona, C.; Galán, M.; Angulo, G.; Muñoz, M. A.; Guardado, P.; Balón, M. *Phys. Chem. Chem. Phys.* **2000**, *2*, 5076.

(23) Chou, P. T.; Liu, Y. I.; Wu, G. R.; Shiao, M. Y.; Yu, W. S.; Cheng, C. C.; Chang, C. P. *J. Phys. Chem. B* **2001**, *105*, 10674.

(24) Inuzuka, K.; Fujimoto, A. *Spectrochim. Acta* **1986**, *42A*, 929.

(25) Konijnenberg, J.; Ekelmans, A. H.; Varma, C. A. G. O. *J. Chem. Soc., Faraday Trans. 2* **1989**, *85*, 1539.

(26) Ishikawa, H.; Iwata, K.; Hamaguchi, H. *J. Phys. Chem. A* **2002**, *106*, 2305.

(27) Frisch, M. J.; Trucks, G. W.; Schlegel, H. B.; Scuseria, G. E.; Robb, M. A.; Cheeseman, J. R.; Zakrzewski, V. G.; Montgomery, J. A., Jr.; Stratmann, R. E.; Burant, J. C.; Dapprich, S.; Millam, J. M.; Daniels, A. D.; Kudin, K. N.; Strain, M. C.; Farkas, O.; Tomasi, J.; Barone, V.; Cossi, M.; Cammi, R.; Mennucci, B.; Pomelli, C.; Adamo, C.; Clifford, S.; Ochterski, J.; Petersson, G. A.; Ayala, P. Y.; Cui, Q.; Morokuma, K.; Malick, D. K.; Rabuck, A. D.; Raghavachari, K.; Foresman, J. B.; Cioslowski, J.; Ortiz, J. V.; Stefanov, B. B.; Liu, G.; Liashenko, A.; Piskorz, P.; Komaromi, I.; Gomperts, R.; Martin, R. L.; Fox, D. J.; Keith, T.; Al-Laham, M. A.; Peng, C. Y.; Nanayakkara, A.; Gonzalez, C.; Challacombe, M.; Gill, P. M. W.; Johnson, B. G.; Chen, W.; Wong, M. W.; Andres, J. L.; Head-Gordon, M.; Replogle, E. S.; Pople, J. A. *Gaussian 98*, revision A.7; Gaussian, Inc.: Pittsburgh, PA, 1998.

(28) Hehre, W. J.; Radom, L.; Schleyer, P. v. R.; Pople, J. A. *Ab initio Molecular Orbital Theory*; John Wiley & Sons: New York, 1986.

(29) (a) Szabo, A.; Ostlund, N. S. *Modern Quantum Chemistry*; McGraw-Hill: New York, 1989 and references therein. (b) Foresman, J. B.; Frisch, A. *Exploring Chemistry with Electronic Structure Methods*, 2nd ed.; Gaussian Inc.: Pittsburgh, PA, 1996.

(30) Frisch, M. J.; Head-Gordon, M.; Pople, J. A. *Chem. Phys. Lett.* **1990**, *166*, 275.

(31) Frisch, M. J.; Head-Gordon, M.; Pople, J. A. *Chem. Phys. Lett.* **1990**, *166*, 281.

(32) Becke, A. D. *J. Chem. Phys.* **1993**, *98*, 5648.

(33) Parr, R. G.; Yang, W. *Density-functional theory of atoms and molecules*; Oxford University Press: New York, 1989.

(34) Petersson, G. A.; Al-Laham, M. A. *J. Chem. Phys.* **1991**, *94*, 6081.

(35) Clark, T.; Chandrasekhar, J.; Spitznagel, G. W.; Schleyer, P. v. R. *J. Comput. Chem.* **1983**, *4*, 294.

(36) Foresman, J. B.; Head-Gordon, M.; Pople, J. A.; Frisch, M. J. *J. Phys. Chem.* **1992**, *96*, 135.

(37) (a) Bauernschmitt, R.; Ahlrichs, R. *Chem. Phys. Lett.* **1996**, *256*, 454. (b) Casida, M. E.; Jamorski, C.; Casida, K. C.; Salahub, D. R. *J. Chem. Phys.* **1998**, *108*, 4439.

(38) Stewart, J. J. P. *J. Comput. Chem.* **1989**, *10*, 221.

(39) Buemi, G. *THEOCHEM* **1988**, *41*, 379.

(40) Bliznyuk, A. A.; Voityuk, A. A. *THEOCHEM* **1983**, *41*, 343.

(41) Cramer, C. J.; Truhlar, D. G. *J. Am. Chem. Soc.* **1993**, *115*, 8810.

(42) Cramer, C. J.; Truhlar, D. G. *J. Comput. Chem.* **1992**, *13*, 1089.

(43) Hawkins, G. D.; Lynch, G. C. *QCPE* **1995**, 606.

(44) Wang, J.; Boyd, R. *J. Phys. Chem.* **1996**, *100*, 16141.

(45) Pimentel, G. C., McClellan, A. L., Eds. *The Hydrogen Bond*; W. H. Freeman: San Francisco;1960; p 368.

(46) In general, it is difficult to distinguish the mechanism between proton transfer and hydrogen atom transfer reactions. Here, we simply adopted the conventional term namely "proton transfer" throughout the text, which is particularly more suitable in describing the sequential double proton-transfer reaction in the later sections.

(47) Jeffrey, G. A. *An Introduction to Hydrogen Bonding*; Oxford University Press: New York, 1997; pp 11−16.

(48) Desiraju, G. R.; Steiner, T. *The Weak Hydrogen Bond in Structural Chemistry and Biology*; Oxford University Press: New York, 1999; pp 50−56.

(49) Full, J.; González, L.; Daniel, C. *J. Phys. Chem. A* **2001**, *105*, 184.

(50) The upgrade of computation facility is currently in progress in order to perform the CASSCF calculation on the relatively large system like the 2AP/acetic acid complex.